International Journal of Applied Engineering Research ISSN 0973-4562 Volume 14, Number 14 (2019) pp. 3242-3251

Combined Effects on MHD Convective Flow Over an Infinite Vertical Porous Plate

L.Rajendra Prasad[1*] and G.Viswanatha Reddy[2]

[1]*Research Scholar, Department of Mathematics, Rayalaseema University, Kurnool, Andhra Pradesh, India 518007.*

[2]*Professor, Department of Mathematics, Sri Venkateswara University, Tirupathi, Andhra Pradesh, India 517502.*

Abstract

We have studied the steady MHD convective two dimensional flow of an incompressible and electrically conducting viscous fluid past an infinite vertical porous plate taking Hall, Soret and Joules dissipation effects into account. The non-dimensional equations are then solved analytically using perturbation technique. With the help of graphs, the effects of the various non-dimensional parameters on velocity, temperature and concentration distributions within the boundary layer are examined. Also the effects of the pertinent parameters on the skin-friction coefficient and rates of heat and mass transfer in terms of the Nusselt and Sherwood numbers are computationally discussed.

Keywords: Hall effects, Heat source; Soret number; Porous medium; Joules dissipation; MHD; Chemical reaction.

1. INTRODUCTION

Applications in biomedical engineering include cardiac MRI, ECG, etc. The mechanism of conduction in ionized gases in the presence of a strong magnetic field is different from that in a metallic substance. The electric current in ionized gases is generally carried by electrons which undergo successive collisions with other charged or neutral particles. In the ionized gases, the current is not proportional to the applied potential except when the electric field is very weak. However, in the presence of a strong electric field, the electrical conductivity is affected by the magnetic field. Consequently, the conductivity parallel to the electric field is reduced. Hence, the current is reduced to the direction normal to both electric and magnetic fields. This phenomenon is known as the Hall effect. The effect of Hall current on MHD flows has been studied by many researchers due to the application of such studies in the problems of MHD generators and Hall accelerators. Datta and Jana [1] studied the Hall current effects on oscillatory magneto-hydrodynamic flow past a flat plate. Biswal and Sahoo [2] presented the Hall current effects on oscillatory hydro-magnetic free convective flow of a visco-elastic fluid past an infinite vertical porous flat plate with mass transfer. Watanabe and Pop [3] presented Hall effects on a magnetohydrodynamic (MHD) boundary layer flow over a continuous moving flat plate. Aboeldahab and Elbarbary [4] studied the Hall current effect on a magneto-hydrodynamic free convection flow past a semi-infinite vertical plate with mass transfer. The Hall current effect with simultaneous thermal and mass diffusion on an unsteady hydro-magnetic flow near an accelerated vertical plate was studied by Acharya *et al.* [5]. Sharma *et al.* [6] presented the Hall effect on MHD mixed convective flow of a viscous incompressible fluid past a vertical porous plate, immersed in a porous medium with heat source/sink. Prabhakar Reddy and Anand Rao [7] presented radiation and thermal diffusion effects on an unsteady MHD free convection mass transfer flow past an infinite vertical porous plate with Hall current and heat source. Raju *et al.* [8] presented the Hall current effects on an unsteady MHD flow between a stretching sheet and an oscillating porous upper parallel plate with constant suction. Recently, Rajput and Kanaujia [9] studied MHD flow past a vertical plate with variable temperature and mass diffusion in the presence of Hall current. Veera Krishna et al. [10] discussed heat and mass transfer on unsteady MHD oscillatory flow of blood through porous arteriole. The effects of radiation and Hall current on an unsteady MHD free convective flow in a vertical channel filled with a porous medium have been studied by Veera Krishna et al. [11]. The heat generation/absorption and thermo-diffusion on an unsteady free convective MHD flow of radiating and chemically reactive second grade fluid near an infinite vertical plate through a porous medium and taking the Hall current into account have been studied by Veera Krishna and Chamkha [12].

In this paper, the steady MHD convective two dimensional flow of an incompressible and electrically conducting viscous fluid past an infinite vertical porous plate taking Hall, Soret and Joules dissipation effects into account.

2. FORMULATION AND SOLUTION OF THE PROBLEM

We consider the mixed convention flow of an incompressible and electrically conducting viscous fluid such that x- axis is taken along the plate in upward direction and z- axis is normal to it (see Fig. 1). The fluid and the plate rotate as a rigid body with a uniform angular velocity about z-axis in the presence of an imposed uniform magnetic field B_0 normal to the plate and taking Hall current into account. Since the motion is two dimensional and length of the plate is large therefore all the physical variables are independent of x. A

International Journal of Applied Engineering Research ISSN 0973-4562 Volume 14, Number 14 (2019) pp. 3242-3251

homogenous first order chemical reaction between fluid and the species concentration is considered in which the rate of chemical reaction is directly proportional to the species concentration.

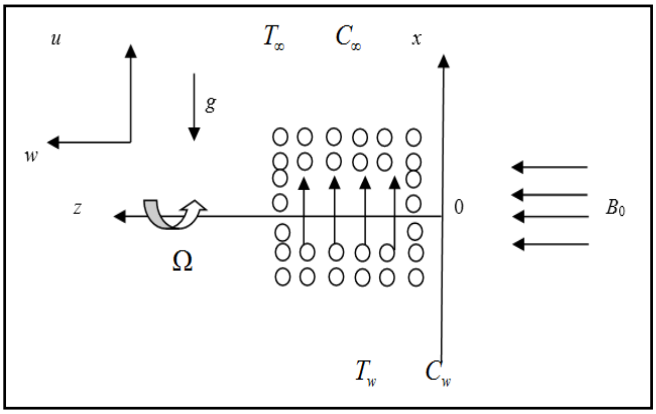

Fig. 1: Physical Configuration of the Problem

The governing equations of continuity, momentum, energy and mass for a flow of an electrically conducting fluid with respect to the rotating frame are

$$\frac{\partial w}{\partial z}=0 \Rightarrow w=-w_0 \ (w_0>0) \tag{1}$$

$$w\frac{\partial u}{\partial z}+2\Omega w=\nu\frac{\partial^2 u}{\partial z^2} +B_0 J_z-\frac{\nu}{k}u+g\beta(T-T_\infty)+g\beta^*(C-C_\infty) \tag{2}$$

$$w\frac{\partial w}{\partial z}-2\Omega u=\nu\frac{\partial^2 w}{\partial z^2}-B_0 J_x-\frac{\nu}{k}w \tag{3}$$

$$w\frac{dT}{dz}=\frac{k_1}{\rho C_p}\frac{d^2T}{dz^2}+\frac{\nu}{C_p}\left(\frac{du}{dz}\right)^2+\frac{\sigma B_0^2}{\rho C_p}(u^2+w^2) +\frac{Q_0}{\rho C_p}(T-T_\infty) \tag{4}$$

$$w\frac{dC}{dz}=D\frac{d^2C}{dz^2}+D_1\frac{d^2T}{dz^2}-k_2(C-C_\infty) \tag{5}$$

The boundary conditions for the velocity, temperature and concentration fields are

$$u=0; w=0; \quad T=T_w; \quad C=C_w \text{ at } z=0 \tag{6}$$

$$u=0; w=0; \quad T\to T_\infty; \quad C\to C_\infty \text{ at } z\to\infty \tag{7}$$

When the strength of the magnetic field is very large, the generalized ohm's law is modified to include the hall current so that

$$J+\frac{\omega_e\tau_e}{B_O}(J\times B)=\sigma\left[E+V\times B+\frac{1}{e\eta_e}\nabla P_e\right] \tag{8}$$

The ion-slip and thermo electric effects are not included in equation (8). Further it is assumed that $\omega_e\tau_e$ ~ 0 (1) and $\omega_i\tau_i << 1$. In equation (8) the electron pressure gradient, the ion-slip and thermo-electric effects are neglected. We also assume that the electric field $E=0$ under assumptions reduces to

$$J_x-m\,J_z=-\sigma B_0 w \tag{9}$$

$$J_z+m\,J_x=-\sigma B_0 u \tag{10}$$

Where $m=\tau_e\omega_e$ is the hall parameter.

On solving equations (9) and (10) we obtain

$$J_x=\frac{\sigma B_0}{1+m^2}(mu-w) \tag{11}$$

$$J_z=\frac{\sigma B_0}{1+m^2}(u+mw) \tag{12}$$

Substituting the equations (11) and (12) in (3) and (2) respectively, we obtain

$$w\frac{\partial u}{\partial v}+2\Omega w=\nu\frac{\partial^2 u}{\partial z^2} +\left(\frac{\sigma B_0^2}{1+m^2}(u+mw)-\frac{\nu}{k}\right)u+g\beta(T-T_\infty) +g\beta^*(C-C_\infty) \tag{13}$$

$$w\frac{\partial w}{\partial z}-2\Omega u=\nu\frac{\partial^2 w}{\partial z^2}-\left(\frac{\sigma B_0^2}{1+m^2}(mu-w)-\frac{\nu}{k}\right)w \tag{14}$$

Combining equations (13) and (14), let $q=u+iw$ we obtain

$$w\frac{\partial q}{\partial v}+2i\Omega q=\nu\frac{\partial^2 q}{\partial z^2}-\left(\frac{\sigma B_0^2}{\rho(1+m^2)}+\frac{\nu}{k}\right)q +g\beta(T-T_\infty)+g\beta^*(C-C_\infty) \tag{15}$$

Introducing following non-dimensional quantities

$$z^*=\frac{zv_0}{\nu}, q^*=\frac{q}{v_0}, \Pr=\frac{\nu\rho C_p}{k}, \theta=\frac{T-T_\infty}{T_w-T_\infty}, \phi=\frac{C-C_\infty}{C_w-C_\infty},$$

$$\text{Gm}=\frac{\nu g\beta^*(C_w-C_\infty)}{v_0^3}, Ec=\frac{v_0^2}{C_p(T_w-T_\infty)}, M^2=\frac{\sigma B_0^2\upsilon}{\rho v_0^2},$$

$$E=\frac{\Omega\nu}{v_0^2}, K=\frac{\nu}{kv_0^2}, \nu=\frac{\mu}{\rho}, \text{Sc}=\frac{\nu}{D}, So=\frac{D_1(T_w-T_\infty)}{\nu(C_w-C_\infty)},$$

$$\text{Gr}=\frac{\nu g\beta(\text{T}_w-\text{T}_\infty)}{v_0^3}, Kr=\frac{\nu k_1}{v_0^2}, Q=\frac{Q_o\nu}{\rho C_p v_0^2}$$

We obtain the governing equations (15), (4) - (5) in the dimensionless form as

$$q''+q'-\left(\frac{M^2}{1+m^2}+\frac{1}{K}+2iE\right)u=-\mathrm{Gr}\theta-\mathrm{Gm}\phi \tag{16}$$

$$\theta''+\Pr\theta'+\Pr Ec(u')^2+\Pr EcM^2(u^2+w^2)+\Pr Q\theta=0 \tag{17}$$

$$\phi''+\mathrm{Sc}\phi'-\mathrm{Sc}Kr\phi+So\mathrm{Sc}\theta''=0 \tag{18}$$

The corresponding boundary conditions in dimensionless form are reduced to

$$q=0;\quad \theta=1;\quad \phi=1 \quad \text{at } z=0 \tag{19}$$

$$q\to 0;\ \theta\to 0;\ \phi\to 0 \quad \text{at } z\to\infty \tag{20}$$

The physical variables q, θ and ϕ can be expanded in the power of Eckert number (Ec). This can be possible physically as Ec for the flow of an incompressible fluid is always less than unity. It can be interrupted physically as the flow due to the Joules dissipation is super imposed on the main flow. Hence we can assume

$$\left.\begin{aligned} q(y)&=q_0(y)+Ecq_1(y)+O(Ec^2)\\ \theta(y)&=\theta_0(y)+Ec\theta_1(y)+O(Ec^2)\\ \phi(y)&=\phi_0(y)+Ec\phi_1(y)+O(Ec^2)\end{aligned}\right\} \tag{21}$$

Using equations (21) in equations (16)-(18) and equating the coefficient of like powers of Ec, we have

$$q_0''+q_0'-\left(\frac{M^2}{1+m^2}+\frac{1}{K}+2iE\right)q_0=-\mathrm{Gr}\theta_0-\mathrm{Gm}\phi_0 \tag{22}$$

$$\theta_0''+\Pr\theta_0'+PrQ\theta_0=0 \tag{23}$$

$$\phi_0''+Sc\phi_0'-KrSc\phi_0=-SoSc\theta_0'' \tag{24}$$

$$q_1''+q_1''-\left(\frac{M^2}{1+m^2}+\frac{1}{K}+2iE\right)q_1=-\mathrm{Gr}\theta_1-\mathrm{Gm}\phi_1 \tag{25}$$

$$\theta_1''+\Pr\theta_1'+\Pr Q\theta_1=-\Pr(u_0')^2-\Pr M^2(u_0^2+w_0^2) \tag{26}$$

$$\phi_1''+\mathrm{Sc}\phi_1'-\mathrm{Sc}Kr\phi_1=-So\mathrm{Sc}\theta_1'' \tag{27}$$

And the corresponding boundary conditions are

$$\begin{aligned}&q_0=0;\quad q_1=0;\quad \theta_0=1;\quad \theta_1=0;\\ &\phi_0=1;\quad \phi_1=0 \quad \text{at} \quad z=0\end{aligned} \tag{28}$$

$$\begin{aligned}&q_0\to 0;\quad q_1\to 0;\quad \theta_0\to 0;\\ &\theta_1\to 0;\quad \phi_0\to 0;\quad \phi_1\to 0 \ \text{ at } \ z\to\infty\end{aligned} \tag{29}$$

Solving equations (22) – (27) with the help of equation (28) – (29), we obtain the velocity, temperature and concentration distribution in the boundary layer.

The skin-friction coefficient at the plate in non-dimensional form is obtained and is given by

$$C_f=\left(\frac{\partial u}{\partial z}\right)_{z=0}$$

The rate of heat transfer coefficient in non-dimensional form is obtained and is given in terms of the Nusselt number, is given by

$$Nu=\left(\frac{\partial \theta}{\partial z}\right)_{z=0}$$

The rate of mass transfer coefficient in non-dimensional form is obtained and is given in terms of the Sherwood number, is given by

$$Sh=\left(\frac{\partial \phi}{\partial z}\right)_{z=0}$$

3. RESULTS AND DISCUSSION:

From the Figs. (2), we noticed that the magnitude of the velocity components *u* and *w* reduces with increasing the intensity of the magnetic field *M*. This is due to the fact that the introduction of a transverse magnetic field, normal to the flow direction, has a tendency to create the drag known as the Lorentz force which tends to resist the flow. The resultant velocity is also reduces with increasing Hartmann number *M*. It is noticed from the Figs. 3, the magnitude of both the velocity components *u* and *w* increases with increasing permeability parameter *K*. Lower the permeability lesser the fluid speed is observed in the entire fluid region. The resultant velocity is also enhances with increasing *K*. The influence of Prandtl number Pr and heat generation parameter *Q* on the dimensionless velocity components *u* and *w* for the fixed values of other parameters is shown in Figs. 4 and 8, respectively. It is noticed that both the dimensionless velocity components *u* and *w* decrease and increase with Pr and *Q*, respectively. The thermal Grashof number Gr signifies the relative effect of the thermal buoyancy force to the viscous hydrodynamic force in the boundary layer. Fig. 5 shows the effects of Gr on the velocity components *u* and *w* for the fixed values of other parameters. It is observed that the dimensionless velocity increases with increasing Gr. The mass Grashof number Gm defines the ratio of the species buoyancy force to the viscous hydrodynamic force. Fig. 6 exhibits the effect of Gm on the dimensionless velocity. It is noticed that the dimensionless velocity increases with increasing Gm. The resultant velocity is also increases with increasing Gr or Gm throughout the fluid region. . Fig. 7 illustrates the effects of chemical reaction parameter Kc on the velocity components *u* and *w* for the fixed values of other parameters. It is observed that the dimensionless velocity slightly decreases with increasing Kc. The resultant velocity is also decreases with increasing Kc throughout the fluid region. Figs. 9 and 10 are prepared to show the influence of Schmidt number Sc and Soret parameter *So* on the dimensionless velocity components *u* and *w*. It is found that there is decrease and an increase in the both dimensionless velocity components *u* and *w* with Sc and *So*, respectively. The resultant velocity is also decreases and increases with increasing Sc and *So* throughout the fluid region. From Figs. 11 both the velocity components *u* and *w* enhance with increasing Hall parameter *m*. The resultant velocity is also increases with increasing Hall parameter throughout the fluid region. The similar behaviour is observed with increasing rotation parameter *E* (Figs. 12).

The persuade of Prandtl number Pr and heat generation parameter *Q* on the dimensionless temperature for the fixed values of other parameters is shown in Figs. 13, respectively. The temperature reduces with increasing Prandtl number Pr and enhances with increasing heat generation parameter *Q*. Fig. 14 displays the result of the dimensionless concentration for various values of chemical reaction parameter Kc, Schmidt number Sc and Soret parameter *So* and Eckert number *Ec*. It is obvious from the figure that the concentration profiles decreases with the increase of Kc. This shows that the buoyancy effects (due to concentration and temperature difference) are important in the plate. Moreover it is observed that the fluid motion is retarded on the account of chemical reaction. This shows that the destructive reaction Kc > 0 leads to fall in the concentration field which in turn weakens the buoyancy effects due to concentration gradients. It is found that there is decrease and an increase in the concentration with increasing Sc and *So* or *Ec*, respectively.

The variation in skin-friction coefficient, the rate of heat transfer in the form of Nusselt number and the rate of mass transfer in the form of Sherwood number for various parameters are studied through Tables 1–3. Skin friction coefficient reduce with increasing Hartmann number M, Prandtl number Pr, chemical reaction parameter Kc and Schmidt number Sc; likewise it enhance permeability parameter K, thermal Grashof number Gr, mass Grashof number Gm, heat generation parameter *Q* and soret parameter *So*(Table 1). The magnitude of the Nusselt number Nu increase with increasing Prandtl number Pr and reduces with increasing heat generation parameter *Q* (Table 2). Similarly the magnitude of the Sherwood number Sh increase with increasing Schmidt number Sc or Chemical reaction parameter Kc and reduces with increasing Soret parameter *So*. For the validity of our work we have compared our results with the existing results of Reddy et al. [25] in the absence of porous medium and heat source. Our result appears to be in excellent agreement with the existing results (Table 4).

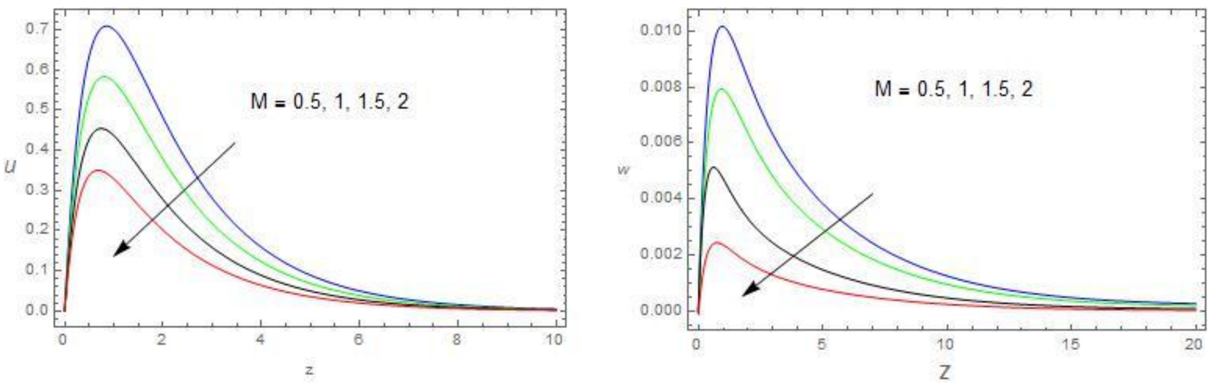

Fig. 2 The velocity profiles for *u* and *w* against *M*
$K=0.5, \mathrm{Pr}=0.71, \mathrm{Gr}=3, \mathrm{Gm}=1, Q=0.1, \mathrm{Kc}=1, \mathrm{Sc}=0.22, So=0.5, m=1, E=0.5$

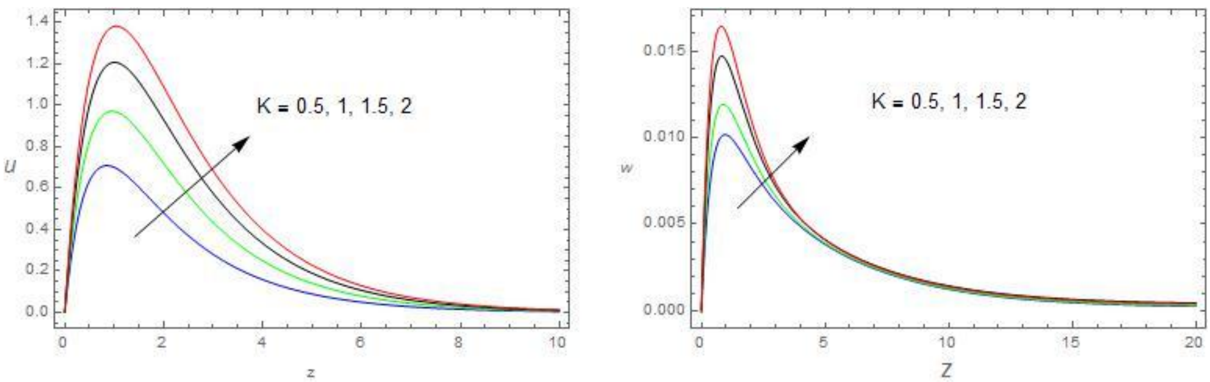

Fig. 3 The velocity profiles for *u* and *w* against *K*
$M=0.5, \mathrm{Pr}=0.71, \mathrm{Gr}=3, \mathrm{Gm}=1, Q=0.1, \mathrm{Kc}=1, \mathrm{Sc}=0.22, So=0.5, m=1, E=0.5$

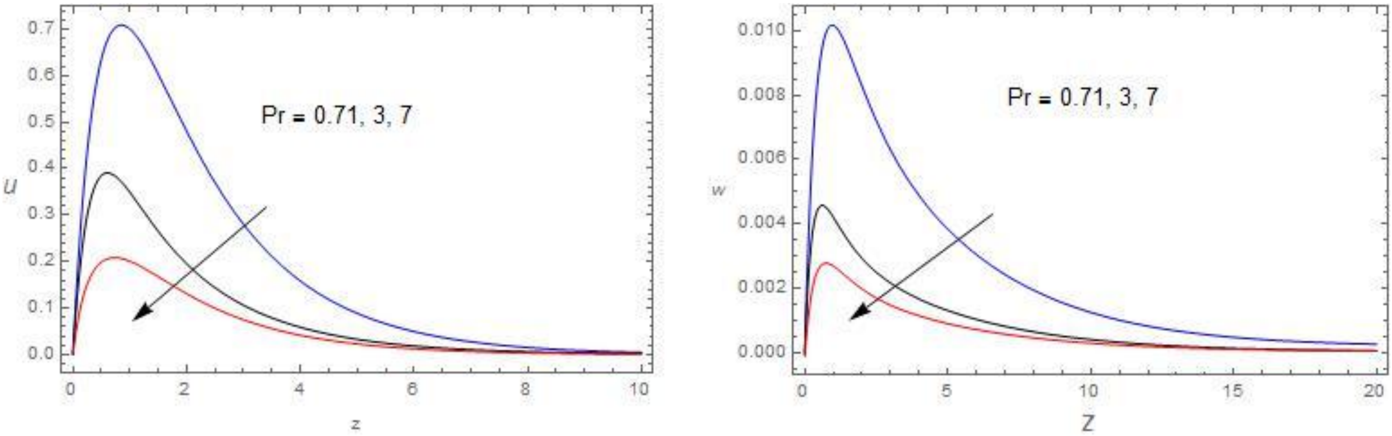

Fig. 4 The velocity profiles for *u* and *w* against Pr
$M=0.5, K=0.5, \mathrm{Gr}=3, \mathrm{Gm}=1, Q=0.1, \mathrm{Kc}=1, \mathrm{Sc}=0.22, So=0.5, m=1, E=0.5$

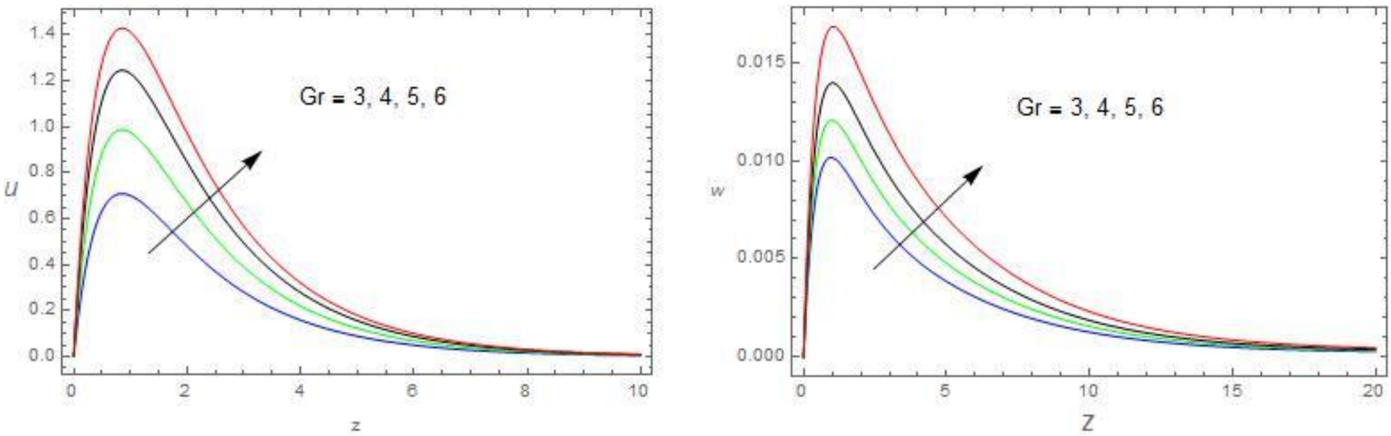

Fig. 5 The velocity profiles for *u* and *w* against Gr
$M=0.5, K=0.5, \mathrm{Pr}=0.71, \mathrm{Gm}=1, Q=0.1, \mathrm{Kc}=1, \mathrm{Sc}=0.22, So=0.5, m=1, E=0.5$

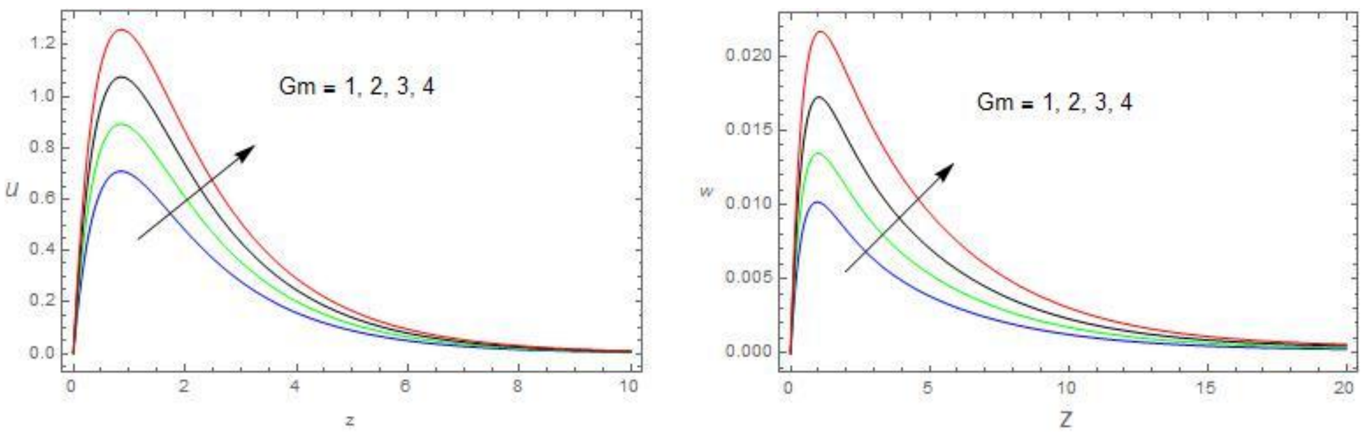

Fig. 6 The velocity profiles for *u* and *w* against Gm
$M=0.5, K=0.5, \mathrm{Pr}=0.71, \mathrm{Gr}=3, Q=0.1, \mathrm{Kc}=1, \mathrm{Sc}=0.22, So=0.5, m=1, E=0.5$

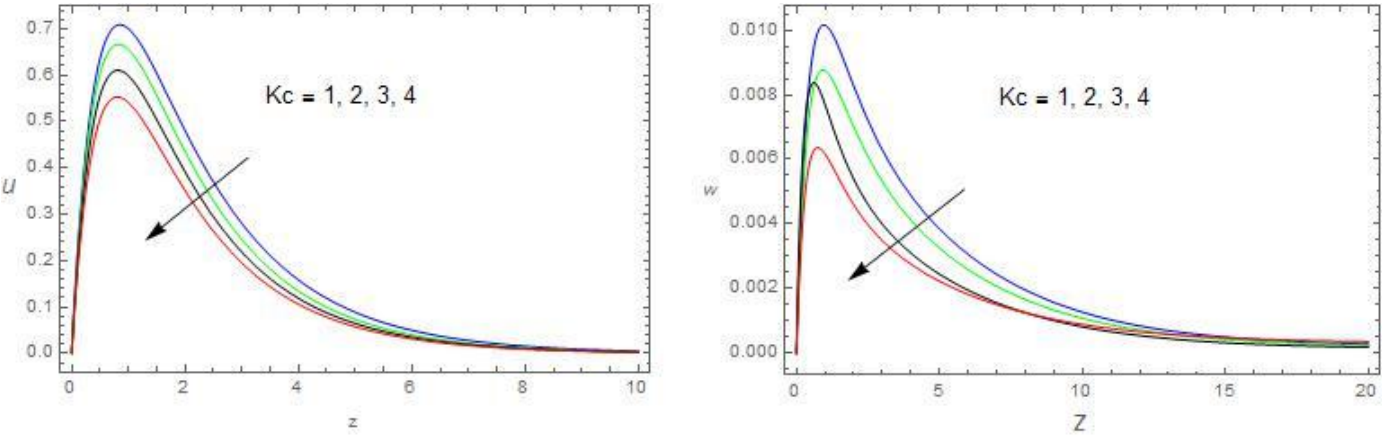

Fig. 7 The velocity profiles for *u* and *w* against Kc
$M=0.5, K=0.5, \mathrm{Pr}=0.71, \mathrm{Gr}=3, \mathrm{Gm}=1, Q=0.1, \mathrm{Sc}=0.22, So=0.5, m=1, E=0.5$

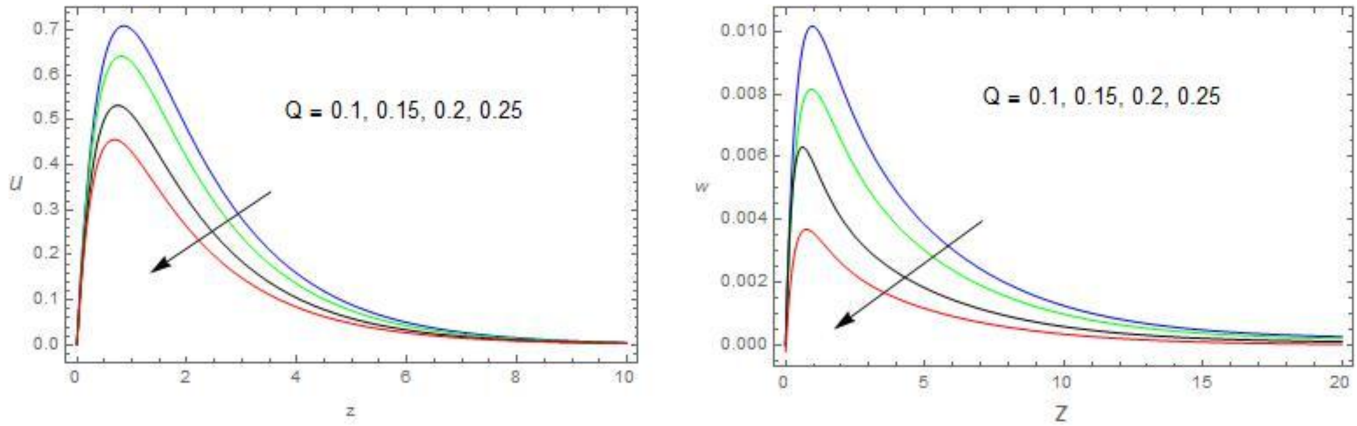

Fig. 8 The velocity profiles for *u* and *w* against *Q*
$M=0.5, K=0.5, \mathrm{Pr}=0.71, \mathrm{Gr}=3, \mathrm{Gm}=1, \mathrm{Kc}=1, \mathrm{Sc}=0.22, So=0.5, m=1, E=0.5$

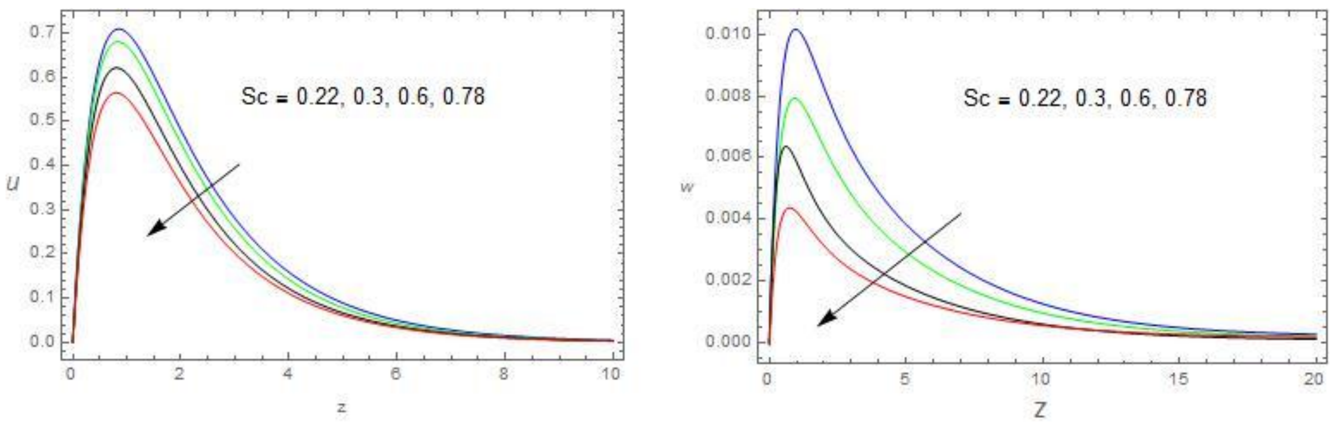

Fig. 9 The velocity profiles for *u* and *w* against Sc
$M=0.5, K=0.5, \mathrm{Pr}=0.71, \mathrm{Gr}=3, \mathrm{Gm}=1, Q=0.1, \mathrm{Kc}=1, So=0.5, m=1, E=0.5$

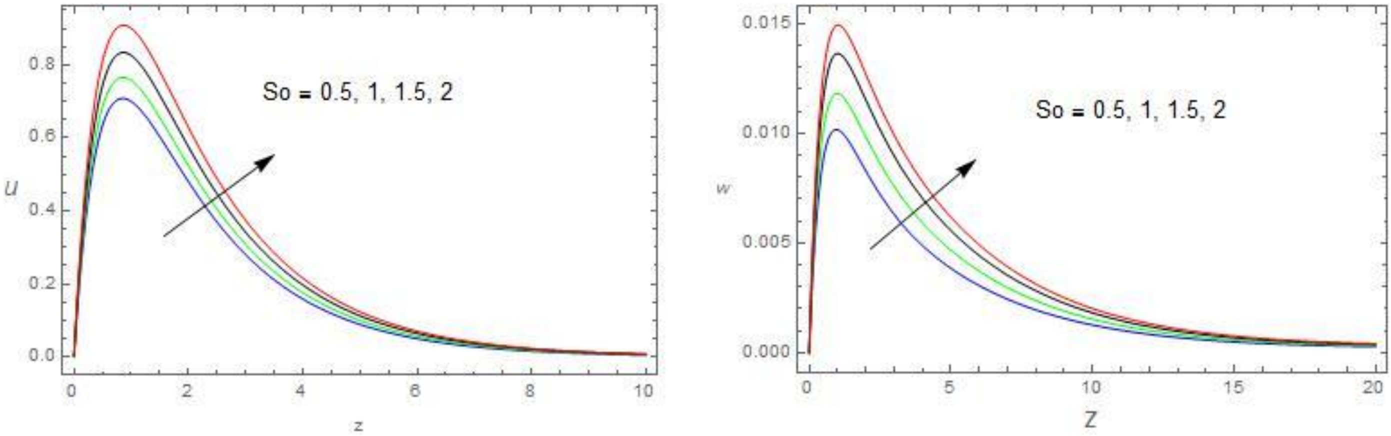

Fig. 10 The velocity profiles for *u* and *w* against *So*
$M=0.5, K=0.5, \mathrm{Pr}=0.71, \mathrm{Gr}=3, \mathrm{Gm}=1, Q=0.1, \mathrm{Kc}=1, \mathrm{Sc}=0.22, m=1, E=0.5$

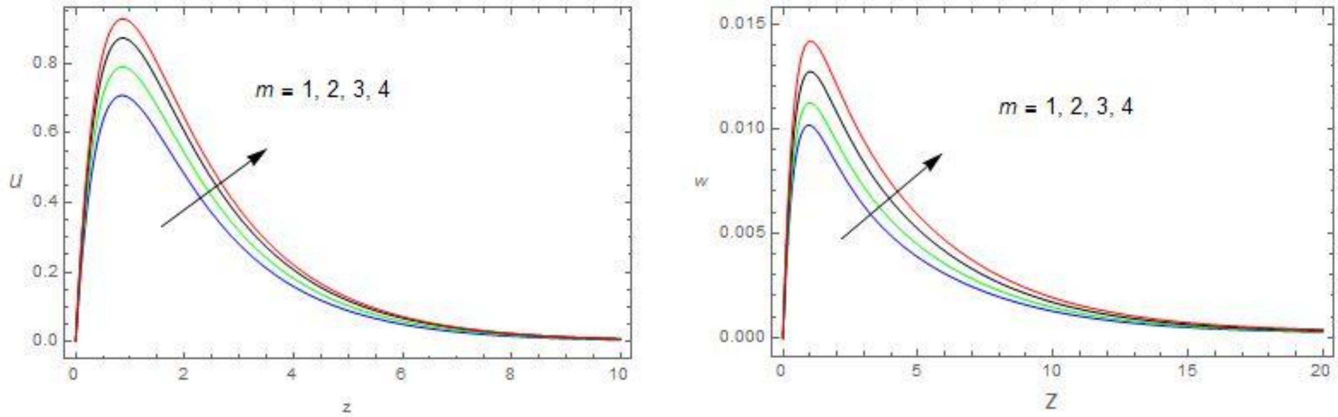

Fig. 11 The velocity profiles for *u* and *w* against *m*
$M=0.5, K=0.5, \mathrm{Pr}=0.71, \mathrm{Gr}=3, \mathrm{Gm}=1, Q=0.1, \mathrm{Kc}=1, \mathrm{Sc}=0.22, So=0.5, E=0.5$

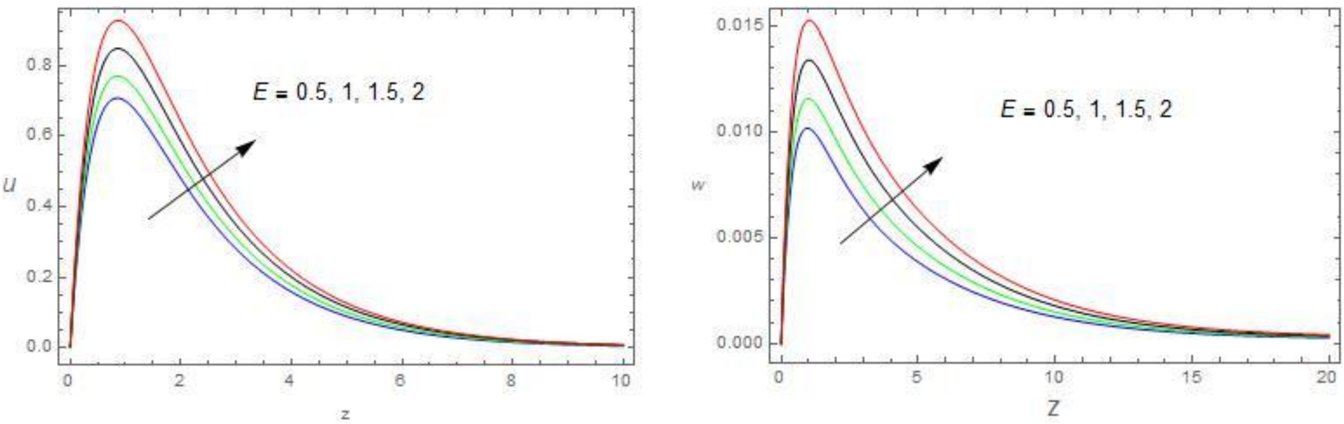

Fig. 12 The velocity profiles for *u* and *w* against *E*
$M=0.5, K=0.5, m=1, \mathrm{Pr}=0.71, \mathrm{Gr}=3, \mathrm{Gm}=1, Q=0.1, \mathrm{Kc}=1, \mathrm{Sc}=0.22, So=0.5$

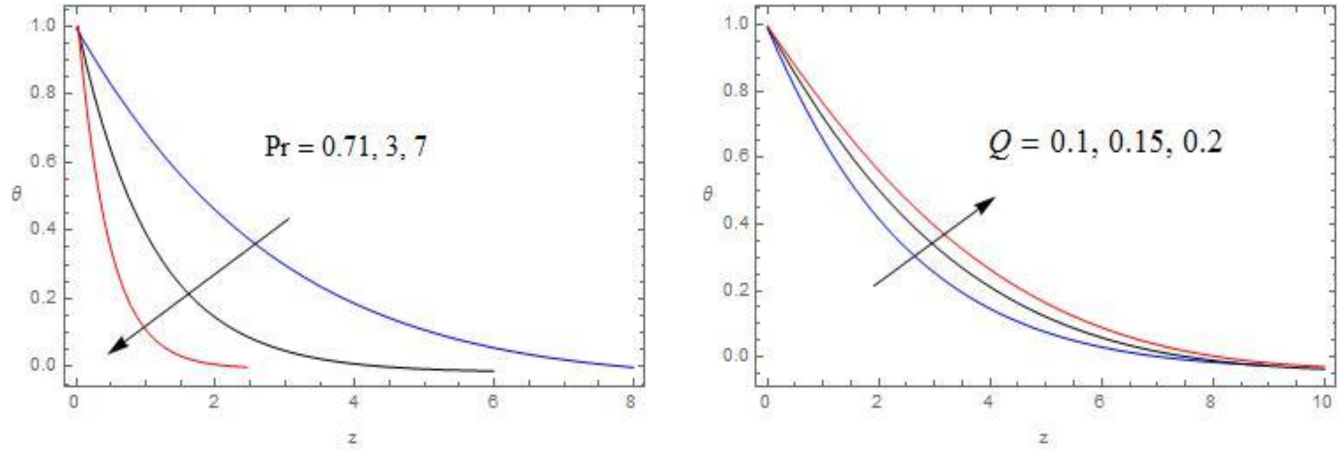

Fig. 13 The temperature profile for θ against Pr and Q

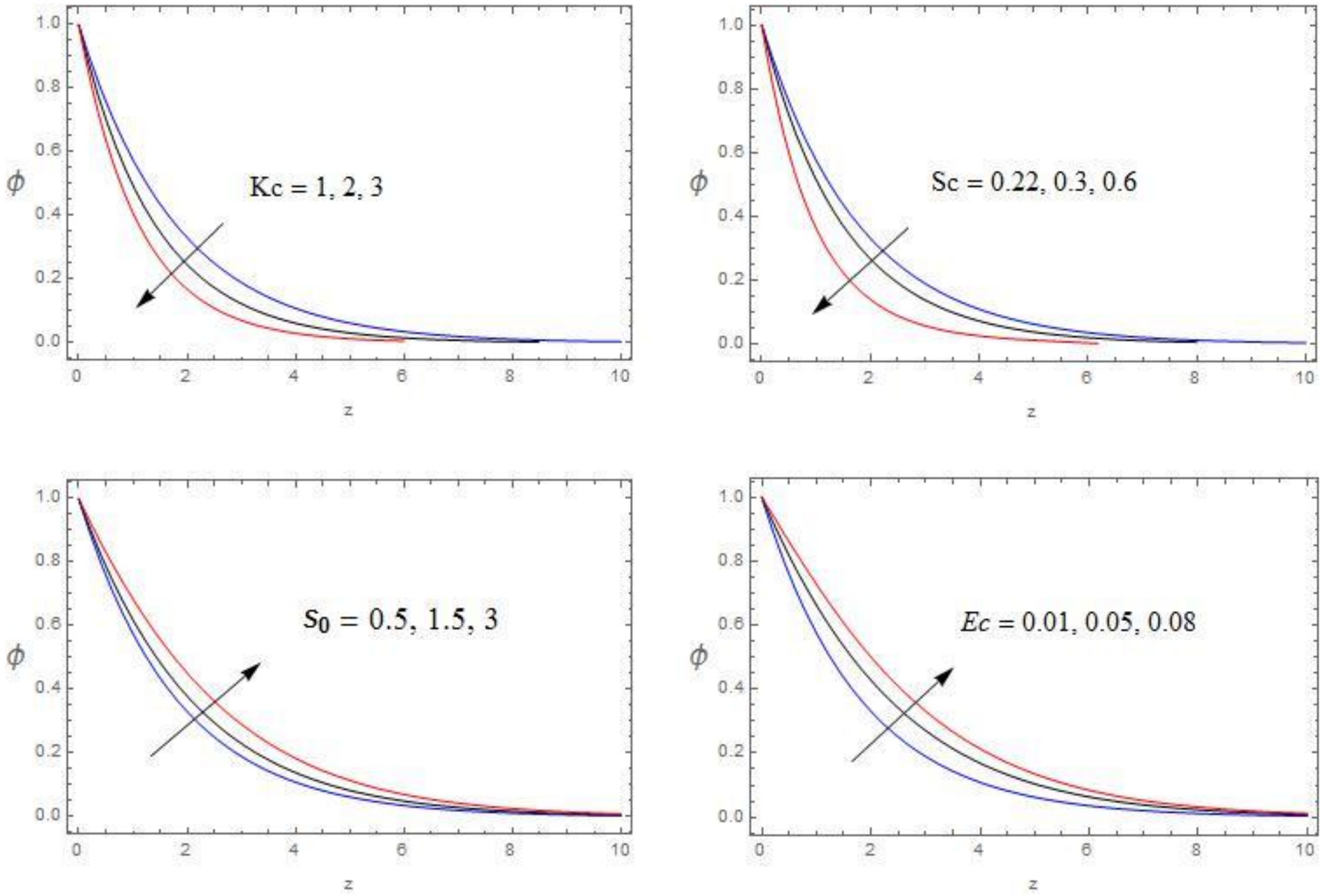

Fig. 14 The Concentration profiles for ϕ against Kc, Sc, *So* and *Ec*

Table 1. Shear stress $(Ec = 0.01)$

M	K	Pr	Gr	Gm	Kc	Q	Sc	So	m	$\|\tau\|$
0.5	0.5	0.71	3	1	1	0.1	0.22	0.5	1	2.42569
1										2.10589
1.5										1.82566
	1									3.08859
	1.5									3.47985
		3								1.39968
		7								1.03025
			4							3.01879
			5							3.62566
				2						3.03025
				3						3.64588
					2					2.35899
					3					2.31477
						0.5				2.69802
						0.8				2.81238
							0.3			2.38996
							0.6			2.28559
								1		2.43669
								1.5		2.45884
									2	2.66338
									3	2.89965

Table 2. Nusselt number
$(M = 0.5, K = 0.5, \mathrm{Gr} = 3, \mathrm{Gm} = 1, \mathrm{Kc} = 1, So = 0.5, \mathrm{Sc} = 0.22, Ec = 0.01)$

Pr	Q	Nu
0.71	0.1	-0.579521
3		-3.009720
7		-6.910550
	0.2	-0.342134
	0.3	-0.133423

Table 3. Sherwood number
$(M = 0.5, K = 0.5, \mathrm{Pr} = 0.71, \mathrm{Gr} = 3, \mathrm{Gm} = 1, Q = 0.1, \mathrm{Kc} = 1, Ec = 0.01)$

So	Sc	Kc	Sh
0.5	0.22	1	-0.553031
1			-0.514333
1.5			-0.475675
	0.3		-0.667466
	0.6		-1.033987
		2	-0.750102
		3	-0.901226

Table 4 Comparison of results with Reddy et al. [25] for $(K = \infty, m = 0, \mathrm{Gr} = 3, \mathrm{Gm} = 1, \mathrm{Pr} = 0.71, Q = 0, Ec = 0.01)$

M	**Kc**	***So***	**Sc**	**Reddy et al. [13]**			**Present work**		
				Cf	**Nu**	**Sh**	**Cf**	**Nu**	**Sh**
0.5	1	0.5	0.22	4.70415	-0.65747	-0.54588	4.70417	-0.65742	-0.54587
1				3.15452	-0.68073	-0.54341	3.15455	-0.68077	-0.54344
1.5				2.30347	-0.69218	-0.54326	2.30346	-0.69216	-0.54328
	2			4.41999	-0.66541	-0.74314	4.41997	-0.66540	-0.74313
	3			4.26892	-0.66922	-0.89451	4.26891	-0.66925	-0.89457
		1		4.77844	-0.65518	-0.50049	4.77841	-0.65516	-0.50042
		1.5		4.85268	-0.65281	-0.45540	4.85266	-0.65284	-0.45544
			0.3	4.52842	-0.66246	-0.65738	4.5285	-0.66245	-0.65739
			0.6	4.19354	-0.67098	-1.01922	4.19356	-0.67099	-1.01921

4. CONCLUSIONS

1. Soret effect increased the concentration of the fluid while chemical effect decreased.
2. The resultant velocity increases with an increase in *m* or Gr or Gm.
3. As the magnetic field parameter *M* increases, the resultant velocity decreases.
4. Both the resultant velocity and concentration of fluid decrease with increase of Schmidt number.
5. An increase in Prandtl number results in the decrease in temperature distribution.
6. Both the resultant velocity and dimensionless temperature are increasing according to the increasing values of heat source parameter.
7. Skin friction coefficient decreases with an increase in *M* or *K*, whereas it shows reverse effect in the case of Gr and Gm.

REFERENCES:

[1]. Datta N. and Jana R.N. (1976), Oscillatory magneto-hydrodynamic flow past a flat plate with Hall effects, J. of Physical Society of Japan, vol.40, No.5, pp.1469-1474.

[2]. Biswal S. and Sahoo P.K. (1994), Hall effect on oscillatory hydro-magnetic free convective flow of a visco-elastic fluid past an infinite vertical porous flat plate with mass transfer, Proc. Nat. Acad. Sci, vol.69A, pp.46-52.

[3]. Watanabe T. and Pop I. (1995), Hall effects on magneto-hydrodynamic boundary layer flow over a continuous moving flat plate, Acta Mechanica, vol.108, No.1, pp.35-47.

[4]. Aboeldahab E.M. and Elbarbary E.M.E. (2001), Hall current effect on MHD free convection flow past a semi-infinite vertical plate with mass transfer, Int. J. Eng. Science, vol.39, pp.1641-1652.

[5]. Acharya M., Dash G.C. and Singh L.P. (2001), Hall effect with simultaneous thermal and mass diffusion onunsteady hydro-magnetic flow near an accelerated vertical plate. Indian J. of Physics, vol.75B, No.1, pp.168-176.

[6]. Sharma B.K., Jha A.K and Chaudhary R.C. (2007), Hall effects on MHD mixed convective flow of a viscous incompressible fluid past a vertical porous plate, immersed in a porous medium with heat source/sink, Rom. Journal Phys, vol.52, No.5-7, pp.487-503.

[7]. Prabhakar Reddy B. and Anand Rao J. (2011), Radiation and thermal diffusion effects on an unsteady MHD free convection mass transfer flow past an infinite vertical porous plate with Hall current and heat source, J. of Eng. Phys. and Thermophysics, vol.84, No.6, pp.1369-1378.

[8]. Raju M.C. Varma S.V.K. and Ananad Reddy N. (2011), Hall current effects on unsteady MHD flow between stretching sheet and an oscillating porous upper parallel plate with constant suction, Thermal Science, vol.15, No.2, pp.45-48.

[9]. Rajput U.S. and Neetu Kanaujia (2016), MHD flow past a vertical plate with variable temperature and mass diffusion in the presence of Hall current, Int. J. of Applied Sci. and Eng., vol.14, No.2, pp.115-123.

[10]. Veera Krishna.M., B.V.Swarnalathamma and J. Prakash, Heat and mass transfer on unsteady MHD Oscillatory flow of blood through porous arteriole, Applications of Fluid Dynamics, Lecture Notes in Mechanical Engineering, vol. XXII, pp. 207-224, 2018. Doi: 10.1007/978-981-10-5329-0_14.

[11]. Veera Krishna.M, G.Subba Reddy, A.J.Chamkha (2018), Hall effects on unsteady MHD oscillatory free convective flow of second grade fluid through porous medium between two vertical plates, Physics of Fluids, vol. **30**, 023106 doi: 10.1063/1.5010863.

[12]. Veera Krishna.M, A.J.Chamkha (2018), Hall effects on unsteady MHD flow of second grade fluid through porous medium with ramped wall temperature and ramped surface concentration, Physics of Fluids **30**, 053101, doi: 10.1063/1.5025542

[13]. Reddy N Anada, Varma SVK, Raju MC. Thermo-diffusion and chemical effects with simultaneous thermal and mass diffusion in MHD mixed convection flow with ohmic heating. J Naval Architect Mar Eng 2009;6, pp. 84-3.